Microencapsulation structures based on protein-coated liposomes obtained through electrospraying for the stabilization and improved bioaccessibility of curcumin

Laura G. Gómez-Mascaraque[1], Caroline Casagrande Sipoli[2], Lucimara Gaziola de La Torre[2], Amparo López-Rubio[1,*]

[1]Food Quality and Preservation Department, IATA-CSIC, Avda. Agustin Escardino 7, 46980 Paterna, Valencia, Spain

[2] School of Chemical Engineering, University of Campinas, UNICAMP, P.O. Box 6066, 13083-970, Campinas-SP, Brazil

*Corresponding author: Tel.: +34 963900022; fax: +34 963636301

E-mail addresses: lggm@iata.csic.es (L. G. Gómez-Mascaraque), latorre@feq.unicamp.br (L. Gaziola de La Torre), carolinesipoli@gmail.com (C. Casagrande Sipoli), amparo.lopez@iata.csic.es (A. López-Rubio)

ABSTRACT

Novel food-grade hybrid encapsulation structures based on the entrapment of phosphatidylcholine liposomes within a WPC matrix through electrospraying were developed and used as delivery vehicles for curcumin. The loading capacity and encapsulation efficiency of the proposed system was studied, and the suitability of the approach to stabilize curcumin and increase its bioaccessibility was assessed. Results showed that the maximum loading capacity of the liposomes was around 1.5% of curcumin, although the loading capacity of the hybrid microencapsulation structures increased with the curcumin content by incorporation of curcumin microcrystals upon electrospraying. Microencapsulation of curcumin within the proposed hybrid structures significantly increased its bioaccessibility (~1.7-fold) compared to the free compound, and could successfully stabilize it against degradation in PBS (pH = 7.4). The proposed approach thus proved to be a promising alternative to produce powder-like functional ingredients.

KEYWORDS

Electrospraying; liposome; encapsulation; curcumin; functional food; bioaccessibility

Chemical compounds studied in this article:

Curcumin (PubChem CID: 969516)

1. Introduction

Curcumin, whose chemical structure is depicted in Figure S1 of the Supplementary Material, is a multivalent compound with attributed antioxidant, antiinflamatory and antimutagenic activities (Changguo Chen, Thomas D. Johnston, Hoonbae Jeon, Roberto Gedaly, Patrick P. McHugh, Thomas G. Burke, et al., 2009) and, thus, an attractive bioactive ingredient for the development of functional foods. However, its poor solubility in water and its great chemical instability (Schneider, Gordon, Edwards, & Luis, 2015) result in very low bioavailability rates upon oral consumption (W. Liu, Zhai, Heng, Che, Chen, Sun, et al., 2016). These drawbacks limit the direct application of curcumin not only in the food industry but also in the medical field (Chin, Huebbe, Pallauf, & Rimbach, 2013; Nelson, Dahlin, Bisson, Graham, Pauli, & Walters, 2017). Hence, a number of strategies have been proposed to design appropriate delivery vehicles for this compound (Feng, Zhu, Chu, Teng, Meng, Deng, et al., 2016; Ndong Ntoutoume, Granet, Mbakidi, Brégier, Léger, Fidanzi-Dugas, et al., 2016).

Liposome dispersions can facilitate the incorporation of lipophilic molecules into food products with a positive impact on their stability and bioavailability (M. Frenzel, Krolak, Wagner, & Steffen-Heins, 2015). Specifically, degradation of curcumin in alkaline conditions can be considerably reduced within liposome environments (El Khoury & Patra, 2013). However, these vehicles have been described to lose entrapped material during storage and to become instable due to osmotic pressure in contact with certain food components such as sugars or salts (Karadag, Özçelik, Sramek, Gibis, Kohlus, & Weiss, 2013; Laye, McClements, & Weiss, 2008). Coating of liposomes with biopolymers has been proposed in a number of works as a plausible strategy to increase their stability and shelf-life (Monika Frenzel & Steffen-Heins, 2015; Gültekin-Özgüven, Karadaı, Duman, Özkal, & Özçelik, 2016; Tan, Feng, Zhang, Xia, & Xia, 2016).

On the other hand, the commercialization of powdery food ingredients is substantially more convenient than handling liquid ingredients such as liposome dispersions, as dried powders are easier to handle and to preserve from contamination during storage and, moreover, they occupy reduced storage volumes (Garti & McClements, 2012). Therefore, biopolymer-coated liposome dry delivery vehicles for food ingredients have been obtained through spray-drying or freeze-drying the corresponding dispersions (M. Frenzel, Krolak, Wagner, & Steffen-Heins, 2015; Van Den Hoven, Metselaar, Storm, Beijnen, & Nuijen, 2012; Wang, Hu, Shen, Xie, Shen, Lu, et al., 2015). However, spray-drying involves the use of high temperatures which can cause degradation of sensitive bioactives (Gómez-Mascaraque & López-Rubio, 2016), and freeze-drying is a considerably expensive technique (Snowman, 1988).

In this context, electrohydrodynamic processing (i.e. electrospinning and electrospraying) has emerged as an alternative drying technique for the production of encapsulation structures under mild conditions by applying a high-voltage electric field to a polymer solution, dispersion or melt (Gómez-Mascaraque, Lagarón, & López-Rubio, 2015). In previous works we have explored this technology to microencapsulate a wide range of bioactive ingredients (Gómez-Mascaraque, Morfin, Pérez-Masiá, Sanchez, & Lopez-Rubio, 2016; Gómez-Mascaraque, Sanchez, & López-Rubio, 2016; Rocio Pérez-Masiá, Lagaron, & Lopez-Rubio, 2015) and it has been recently explored for the encapsulation of β-carotene-loaded liposomes within biodegradable electrospun fibres (de Freitas Zômpero, López-Rubio, de Pinho, Lagaron, & de la Torre, 2015).

In this work, the design of novel food-grade hybrid encapsulation vehicles for curcumin, based on the entrapment of curcumin-loaded liposomes within a protein matrix was proposed, and its impact on the stability and bioaccessibility of curcumin was assessed. The maximum loading capacity of these carriers was also investigated. A

whey protein concentrate was selected as the encapsulation matrix to produce the hybrid capsules. Whey proteins are cheap by-products from the cheese industry with functional characteristics (López-Rubio & Lagaron, 2012) which are electrosprayable in aqueous media (Gómez-Mascaraque, Lagarón, & López-Rubio, 2015; López-Rubio & Lagaron, 2012). They have been already used for liposome coating and have previously shown protective effects when used as encapsulation matrix (Gómez-Mascaraque, Lagarón, & López-Rubio, 2015; R. Pérez-Masiá, López-Nicolás, Periago, Ros, Lagaron, & López-Rubio, 2015).

2. Materials and Methods

2.1. Materials

Whey protein concentrate (WPC), under the commercial name of Lacprodan® DI-8090, was kindly donated by ARLA (ARLA Food Ingredients, Denmark). Pure phosphatidylcholine (98% ± 4%) stabilized with 0.1% ascorbyl palmitate, under the commercial name of Phospholipon® 90G, was obtained from Phospholipid GmbH (Germany). Curcumin (>99.5%), phosphate buffered saline system (PBS, pH = 7.4), pepsin from porcine gastric mucosa, pancreatin from porcine pancreas and bile extract porcine were obtained from Sigma-Aldrich (Spain). Pefabloc® was supplied by Fluka. All inorganic salts used for the *in-vitro* digestion tests were used as received. Absolute ethanol (>99.5%) was purchased from Synth (Brasil), and acetonitrile from Merck (Germany).

2.2. Liposomes production

Liposomes were prepared using the ethanol injection method based on the protocol described in de Freitas Zômpero, López-Rubio, de Pinho, Lagaron, and de la Torre (2015), with modifications. Briefly, phosphatidylcholine ('the lipids') was dispersed in absolute ethanol at room temperature and added dropwise to milliQ water in a volumetric ratio of 10% under continuous stirring at 1336 rpm using a Cowles type impeller. The agitation was maintained for 5 min after the addition of the lipids. Different lipid concentrations were tested, ranging from 20-80 g/L in the final liposome dispersion.

In order to reduce the size of the liposomes the samples were subjected to ultrasonic treatments using a 2 mm ultrasound probe model SXB30 (Sonomax Srl, Italy) in pulse mode (30% active cycle) for 1 min 30 s in intervals of 30 s at increasing power (i.e. 60, 90 and 120 W, respectively). Curcumin-loaded liposomes were produced by adding different amounts of curcumin to the lipids solutions in ethanol, in mass ratios ranging from 1-8% with respect to the lipids.

2.3. Size distribution of the liposomes

The size distribution of the liposomes was determined via dynamic light scattering (DLS) with a Zetasizer Nano ZS (Malvern Instruments Corp., WORCS, UK), according to the method described in Sipoli, Santana, Shimojo, Azzoni, and de la Torre (2015) prior dilution to a lipid concentration of 20 µg/mL with milliQ water, and intensity-weighted results are reported.

2.4. Morphology of the liposomes

Transmission electron microscopy (TEM) was conducted on a LEO 906E microscope (Zeiss, Germany) at 60 kV. Liposome dispersions were diluted to 1 mg/mL lipids and 5 μL of the samples were deposited on 400-mesh copper grids coated with Formvar carbon film. The excess water was removed with blotting paper after 30 s. The samples were subjected to negative staining with 1% (w/v) uranyl acetate prior to examination (5 μL of staining solution was deposited and dried after 10 s).

2.5. Preparation of liposome/protein formulations

WPC (25% w/v) was dispersed in milliQ water at room temperature under vigorous magnetic stirring. The required volume of liposome dispersion was subsequently added to achieve final lipids/WPC mass ratios of 2.5, 5, 7.5 and 10%, under continuous agitation. The final WPC concentration in the formulation was 20% (w/w), as required for the subsequent electrohydrodynamic processing step (Gómez-Mascaraque & López-Rubio, 2016).

2.6. Production of hybrid microencapsulation structures by electrospraying

The previous formulations were processed using a homemade electrospinning/ electrospraying apparatus assembled in-house. The dispersions were pumped with a digitally controlled syringe pump model KDS-100 (KDScientific, USA) at a flow-rate of 0.15 mL/h through a needle with an inner diameter of 0.84 mm. Processed samples were collected on a grounded copper plate covered with aluminium foil which was placed at a distance of 10 cm from the tip of the needle in a horizontal configuration.

155 The applied voltage was 10 kV as selected from preliminary tests in order to attain
156 stable electrospraying.

157

158 **2.7. Morphological characterization of the particles**

159 Scanning electron microscopy (SEM) was conducted on a Leo 440i microscope (LEO
160 Electron Microscopy/Oxford, Cambridge, United Kingdom) at an accelerating voltage
161 of 10 kV and a working distance of 15 mm after sputter-coating the samples with gold.
162 Particle diameters were measured from the SEM micrographs using the ImageJ
163 software. Size distributions were obtained from a minimum of 200 measurements.

164

165 **2.8. Fourier transform infrared (FT-IR) analysis of the samples**

166 FT-IR spectra were collected using a Nicolet 6700 Thermo Scientific FT-IR equipment
167 (USA). The powdery electrosprayed materials were dispersed in spectroscopic grade
168 potassium bromide and analysed in transmission mode. The lipids' spectrum was
169 obtained without further processing in ATR mode. All spectra were obtained by
170 averaging 32-64 scans at 4 cm^{-1} resolution.

171

172 **2.9. Entrapment efficiency within the liposomes**

173 The liposome dispersions were centrifuged at 100×g and 4 °C for 5 min using a Heal
174 Force Neofuge 23R centrifuge (Thanes Science, Thailand). These conditions were
175 optimized in preliminary trials to precipitate the non-encapsulated crystals of curcumin
176 and not the liposomes. The supernatant was diluted 4-fold with ethanol, dissolving the

liposomes and curcumin. The concentration of curcumin was then assessed by UV-vis spectroscopy at 425 nm using a Thermo spectrophotometer model Genesys 6 (New York, USA), prior preparation of a calibration curve (R^2 = 0.9995). The entrapment efficiency (EE) and the loading capacity (LC) of the liposomes were calculated according to Eq. 1 and 2, respectively.

$$EE_{lip}\ (\%) = \frac{Mass\ of\ entraped\ curcumin\ (experimental)}{Total\ mass\ of\ curcumin\ added\ (theoretical)} \cdot 100 \quad \text{Eq. 1}$$

$$LC_{lip}\ (\%) = \frac{Mass\ of\ entraped\ curcumin\ (experimental)}{Total\ mass\ of\ lipids\ in\ the\ liposomes\ (theoretical)} \cdot 100 \quad \text{Eq. 2}$$

2.10. Polarized light microscopy

Polarized light microscopy images were taken using a digital microscopy system (Nikon, Multizoom AZ100, Japan) equipped with a polarized light source (Nikon, C-FI115 Fiber Illuminator, Japan) and a digital camera head (Nikon, DS-Ri1, Japan).

2.11. Differential scanning calorimetry (DSC)

DSC was performed using a differential scanning calorimeter model DSC1 from Mettler Toledo (Switzerland) after freeze-drying the liposome suspensions. The samples (ca. 25 mg) were placed in perforated standard aluminium pans (40 µl) and subjected to a heating ramp from -50 to 200 ºC at a scanning rate of 10 ºC/min under a dynamic nitrogen atmosphere (45 mL/min).

2.12. Encapsulation efficiency within the hybrid encapsulation structures

The electrosprayed materials were dispersed in water (16 mg/mL) and vortex-agitated to disrupt the protein capsules. The dispersions were then slowly diluted 4-fold in ethanol to precipitate WPC while dissolving the lipids and curcumin. After centrifugation at 5000 g and 4 ºC during 20 min, the curcumin concentration in the supernatant was analysed by UV-vis spectroscopy as described above. The encapsulation efficiency (EE) and loading capacity (LC) of the electrosprayed hybrid structures were calculated according to Eq. 3 and 4, respectively.

$$EE_{hyb}\ (\%) = \frac{Mass\ of\ entraped\ curcumin\ (experimental)}{Total\ mass\ of\ curcumin\ added\ (theoretical)} \cdot 100 \qquad \text{Eq. 3}$$

$$LC_{hyb}\ (\%) = \frac{Mass\ of\ entraped\ curcumin\ (experimental)}{Total\ mass\ of\ the\ hybrid\ structures\ (experimental)} \cdot 100 \qquad \text{Eq. 4}$$

2.13. Curcumin degradation assays

Free curcumin, curcumin-loaded liposomes and curcumin-loaded hybrid capsules were dissolved/dispersed in PBS (pH=7.4) to achieve theoretical curcumin concentrations of 0.01 mg/mL in all cases. For free curcumin, a 1 mg/mL stock solution was first prepared in absolute ethanol and subsequently diluted 100-fold in PBS. After selected time intervals, aliquots of the aforementioned solutions/dispersions were diluted 3-fold with absolute ethanol, centrifuged for 30 s at 12000 rpm using an Eppendorf MiniSpin microcentrifuge from Fisher Scientifics and their absorbance at 425 nm was measured as described in section 2.9.

2.14. *In-vitro* gastrointestinal digestion

Suspensions of the curcumin-containing hybrid microcapsules (40 mg/mL) and the equivalent concentration of free curcumin (0.04 mg/mL) in distilled water were subjected to *in-vitro* digestion following the method described by Gómez-Mascaraque, Soler, and Lopez-Rubio (2016). Aliquots collected after the duodenal phases were snap-frozen in liquid nitrogen until further use.

2.15. Bioaccessibility assessment

The amount curcumin released during digestion was estimated after centrifugation of the digestas. The supernatants were freeze-dried, re-suspended in water and extracted with 70 % acetonitrile before HPLC-MS analysis. Eluent A was water slightly acidified with 0.005% acetic acid, and eluent B acetonitrile with 0.005% acetic acid, working in isocratic mode at 70% of eluent B. The LC system used for this analysis was an Acquity® TQD system from Waters. Separation of curcumin was performed using an Acquity UPLC C18 Kinetex (Phenomenex, 100 mm x 2.1 mm, 1.7 µm particle size) LC-column. The flow rate was set to 0.4 mL/min. The injection volume was 5 µl. The mass spectrometer was equipped with a Z-spray electrospray ionization source and spectra were acquired in positive ionization multiple reaction monitoring (MRM) mode with interchannel delay of 0.16 s. The bioaccessibility was estimated according to Eq. 5, where EE_{hyb} refers to the encapsulation efficiency obtained for the hybrid structures (cf. Eq. 3).

$$Bioaccessibility\ (\%) = \frac{[curcumin] in\ digesta}{[curcumin]_{theoretical} \times EE_{hyb}} \cdot 100 \qquad \text{Eq. 5}$$

2.16. Statistical analysis

Significant differences between homogeneous sample groups were obtained through two-sided t-tests at $p < 0.05$ using IBM SPSS Statistics software (v.23) (IBM Corp., USA). For multiple comparisons, the p-values were adjusted using the Bonferroni correction.

3. Results and discussion

3.1. Phosphatidylcholine liposomes

Suspensions of liposomes with different lipid (phosphatidylcholine) concentrations, ranging from 20-80 g/L, were prepared using the ethanol injection method. The size distribution of the obtained liposomes could not be accurately determined by DLS due to their big sizes and great polydispersity index (results not shown). Jaafar-Maalej and co-workers had also observed an increase in the size of liposomes produced using egg-yolk lecithin by ethanol injection when the lipids concentration was increased from 10 g/L to 60 g/L, and the formation of large aggregates when the lipids concentration was higher than 60 g/L (Jaafar-Maalej, Diab, Andrieu, Elaissari, & Fessi, 2010).

Subsequent attempts to electrospray the protein dispersions containing the prepared liposomes failed, as the disturbance of the Taylor cone caused by the big-sized liposomes led to dripping of the dispersions. Therefore, the liposomes were subjected to a ultrasonic treatment (cf. Section 2.2) in order to reduce their size (Yamaguchi, Nomura, Matsuoka, & Koda, 2009) while maintaining high lipids concentrations in the final hybrid structures.

Table 1 summarizes the average size and polydispersity index (intensity weighted) of the obtained liposomes after the ultrasonic treatment. The results showed that both the average size of the liposomes and their polydispersity increased with the lipid concentration. In order to confirm the results from DLS, the liposomes were observed

by transmission electron microscopy (TEM). Figure S2 of the Supplementary Material shows a TEM image obtained for liposomes prepared with a final lipid concentration of 80 g/L, whose sizes are in the range of those obtained by DLS.

3.2. Hybrid electrosprayed capsules

Electrosprayed capsules were obtained from WPC dispersions containing sonicated phosphatidylcholine liposomes produced at different lipid concentrations in order to ascertain whether the concentration and size of the liposomes had an impact on the sprayability of the suspensions and the morphology and size of the obtained encapsulation structures. All evaluated liposome concentrations (i.e. up to a 10% w/w of lipids with respect to the protein) could be successfully electrosprayed, and the images obtained by scanning electron microscopy (SEM) of the capsules are shown in Figure 1, together with their particle size distributions. From these images it was concluded that all the dispersions containing liposomes at different concentrations and with different size distributions yielded spherical capsules upon electrospraying, finding no significant differences in their size distributions. Therefore, the maximum concentration tested, i.e. 10% w/w of lipids with respect to the protein, was selected for further experiments, in order to maximize the amount of bioactive to be incorporated in the hybrid encapsulation structures.

INSERT FIGURE 1 ABOUT HERE

Figure 1 also shows the FT-IR spectra of the capsules containing 10% w/w liposomes, together with the spectrum of WPC capsules containing no lipids and that of the

commercial lipids. The spectrum of electrosprayed WPC in the absence of lipids exhibited the characteristic bands of proteins centered at 3411 cm^{-1} (Amide A, N-H stretching), 3075 cm^{-1} (Amide B, asymmetric stretching of =C-H and NH_3^+), 1650 cm^{-1} (Amide I, C=O and C-N stretching), 1547 cm^{-1} (Amide II, N-H bending) and 1242 cm^{-1} (Amide III, C-N stretching) (Gómez-Mascaraque & López-Rubio, 2016). These bands were also observed in the spectrum of the hybrid capsules, where the presence of lipids within the electrosprayed structures was evidenced by the increase in the intensity of the peaks at 2854 and 2925 cm^{-1} (ascribed to the symmetric and asymmetric vibrational modes of CH_2 groups), the bands at 1242, 1156 and 1079 cm^{-1} (associated to contributions of phosphate groups in the lipids), and the appearance of a shoulder at 1739 cm^{-1} corresponding to the band at 1736 cm^{-1} (vibration of C=O groups) in the pure lipids (Hielscher, Wenz, Hunte, & Hellwig, 2009).

Spectral band shifts were observed in the hybrid capsules with respect to its individual components, such as the band ascribed to the Amide B, which shifted to 3072 cm^{-1} in the hybrid structures, or the mentioned band at 1739 cm^{-1}, which was originally centered at 1736 cm^{-1} in the commercial lipids. The spectral changes corresponding to lipid vibrational bands, have been attributed to the reorganization of their supramolecular structure (Hielscher, Wenz, Hunte, & Hellwig, 2009) upon liposome production. On the other hand, potential intermolecular interactions between the lipids and the protein might be also taking place, as suggested by the shifts observed in the bands ascribed to the protein. Indeed, globular proteins and, in particular, whey proteins, have been described to suffer conformational changes resulting from adsorption to oil droplets in oil-in-water emulsions (Malaki Nik, Wright, & Corredig, 2010; McClements, 2004), consequently exposing their non-polar residues. A similar phenomenon could take place in the prepared liposome dispersions, where the

316 liposomes would act as self-organized oil droplets, which would interact with the
317 exposed non-polar residues of the protein. Previous works have already suggested that
318 phospholipids can modify the secondary structure of whey proteins due to hydrophobic
319 interactions (Kasinos, Sabatino, Vanloo, Gevaert, Martins, & Van der Meeren, 2013),
320 allowing even the insertion of whey proteins into the liposomal membrane (Monika
321 Frenzel & Steffen-Heins, 2015).

322

323 **3.3. Curcumin-loaded liposomes and microcapsules**

324 The selected hybrid carrier, i.e. with a lipid content of 10% w/w, was loaded with
325 different concentrations of curcumin. For this purpose, curcumin-loaded liposomes
326 (lipid concentration of 80 g/L) were first produced by adding different amounts of
327 curcumin (1-8% w/w with respect to the lipids) to the lipid solutions before injection.
328 After mixing with the protein dispersion, the mixture was electrosprayed.

329 Table 1 summarizes the average size and polydispersity index (intensity weighted) of
330 the obtained curcumin-loaded liposomes, which increased with increasing curcumin
331 contents. Being curcumin a lipophilic compound, it was expected to be located in the
332 hydrophobic region of the liposomal bilayer, having an impact on the size and stability
333 of the liposomes. In fact, (Karewicz, Bielska, Gzyl-Malcher, Kepczynski, Lach, and
334 Nowakowska (2011)) reported that liposomes based on egg yolk phosphatidylcholine
335 and dihexadecyl phosphate were destabilized upon loading with curcumin. Similarly,
336 curcumin affected the phase transition of 1,2-dimyristoyl-*sn*-glycero-3-phosphocholine
337 liposomes (El Khoury & Patra, 2013).

338

339 INSERT TABLE 1 ABOUT HERE

340

341 Despite this increase in the size and polydispersity of the liposomes, all the above
342 curcumin-loaded liposomes could be successfully electrosprayed when incorporated in
343 the WPC dispersions, causing no substantial changes in the size and morphology of the
344 hybrid capsules (c.f. Section 3.5).

345

346 **3.3.1. Entrapment of curcumin within the liposomes**

347 In order to ascertain the amount of curcumin effectively incorporated within the
348 liposomes as a function of the curcumin concentration added to the lipids solution, the
349 entrapment efficiency (EE) and loading capacity (LC) of the systems were calculated
350 according to Eq. 1 and 2, respectively. Results are summarized in Table 2.

351 The results showed that the encapsulation efficiency decreased with the amount of
352 curcumin added to the lipids solutions. However, no significant differences were
353 observed in the loading capacity of the samples, regardless of the initial curcumin
354 concentration. Therefore, it was concluded that a maximum curcumin loading of about
355 1.5 % (w/w) with respect to the mass of lipids could be effectively incorporated within
356 the liposomal bilayer. The excess curcumin would then be excluded from the liposomes
357 structure, crystallizing upon contact with water and hence decreasing the entrapment
358 efficiency above the mentioned loading capacity.

359 To confirm this hypothesis, the curcumin-loaded liposomes suspensions were
360 centrifuged and the obtained pellet was observed under a polarized light microscope to
361 corroborate the presence of curcumin microcrystals. The obtained images are shown in

Figure S3 of the Supplementary Material. While very few microcrystals were observed when a proportion of 1% w/w curcumin was used, the concentration and size of the microcrystals tended to increase as more curcumin was incorporated into the lipids solution.

The above qualitative assessment was complemented with DSC measurements. As inferred in Section 3.3, liposomal curcumin is expected to be located in the phospholipid bilayer and impact its stability. Hence, the liposome phase transition associated with the disruption of the phospholipid bilayer was expected to occur at lower temperatures when curcumin was incorporated in the liposomes (El Khoury & Patra, 2013; Patra, El Khoury, Ahmadieh, Darwish, & Tafech, 2012). In fact, a reduction of the transition temperature has been already observed in phosphatidylcholine-based liposomes upon curcumin loading (Y. Liu, Liu, Zhu, Gan, & Le, 2015). It was hypothesized that the decrease in the phase transition temperature (i.e. 'the destabilization') would be proportional to the amount of curcumin incorporated within the liposomal bilayer. Figure 2 shows the DSC thermograms of unloaded and curcumin-loaded freeze-dried liposomes.

INSERT FIGURE 2 ABOUT HERE

Indeed, the obtained thermograms showed that curcumin-loading lowered the transition temperature of the liposomes more than 5 ºC, and small differences were observed amongst the transition temperature of the curcumin-loaded liposomes with different curcumin concentrations, suggesting that the amount of curcumin effectively

385 incorporated in the liposomal bilayer did not differ substantially regardless of the
386 curcumin concentration in the initial lipid solution.
387
388 **3.3.2. Encapsulation efficiency within the hybrid microcapsules**
389 The double encapsulation of curcumin within the hybrid structures was accomplished
390 by incorporating the curcumin-loaded liposome suspensions into WPC dispersions (in a
391 lipid:WPC ratio of 10% w/w and different curcumin:lipid ratios) and electrospraying the
392 mixture as previously done with the unloaded liposomes. Again, spherical capsules
393 were obtained with similar size distributions as those observed in Figure 1. A
394 representative SEM image is shown in Figure S4 of the Supplementary Material for a
395 theoretical curcumin concentration of 0.2% w/w with respect to the protein mass. The
396 curcumin encapsulation efficiency (EE) and the loading capacity (LC) of the hybrid
397 microcapsules were calculated according to Eq. 3 and 4, respectively, for different
398 theoretical curcumin concentrations. The results are summarized in Table 2.
399
400 INSERT TABLE 2 ABOUT HERE
401 As previously observed for the simple liposomal encapsulation, the efficiency of the
402 hybrid encapsulation process decreased as the theoretical curcumin concentration
403 increased. However, the loading capacity of the capsules increased as the curcumin
404 concentration did, and was higher than that expected considering the results in the
405 previous section. Considering the maximum curcumin loading capacity of the liposomes
406 previously calculated of around 1.5%, loading capacities of the hybrid capsules greater
407 than 0.15% would imply that part of the curcumin present in those hybrid structures was
408 not entrapped within the lipids and should then be in crystalline form. Accordingly, the
409 smallest curcumin crystals present in the liposomal dispersion might have remained in

suspension during the electrospraying process, aided by the relatively high viscosity of the WPC dispersion. On the other hand, bigger crystals would have precipitated in the syringe, decreasing the encapsulation efficiency as observed when increasing curcumin concentrations. However, although an increase in the loading capacity of the hybrid capsules was observed upon increasing the curcumin concentration in the solutions, the physical form of the curcumin (either crystalline or liposomal) was expected to have implications in its bioaccessibility and, consequently, in its bioavailability (cf. Section 3.4).

3.4. Bioaccessibility of curcumin after *in-vitro* digestion

The bioaccessibility can be defined as the fraction of a compound 'that is soluble in the gastrointestinal (GI) environment and is available for absorption' or 'the fraction of external dose released from its matrix in the GI tract' (Cardoso, Afonso, Lourenço, Costa, & Nunes, 2015). In particular, the bioaccessibility of lipophilic ingredients has been related to the fraction of the compounds which is incorporated into the mixed micellar phase formed during digestion in the small intestine (Qian, Decker, Xiao, & McClements, 2012). Therefore, in this work the bioaccessibility was calculated as the fraction of the original curcumin content which was recovered from the micellar phase after *in-vitro* digestion (i.e. the clear phase observed after centrifugation of the digestas), as described in previous works (Ahmed, Li, McClements, & Xiao, 2012; Qian, Decker, Xiao, & McClements, 2012). The original curcumin content was calculated taking into account the theoretical loading of the hybrid microcapsules and the encapsulation efficiency, as expressed in Eq. 5. Results are shown in Table 3.

434 INSERT FIGURE 3 ABOUT HERE

435

436 Results showed that the bioaccessibility of pure curcumin was very low, as expected.
437 Microencapsulation of the compound within the proposed hybrid structures, however,
438 significantly increased its bioaccessibility (~1.7-fold), regardless of the curcumin
439 content in the capsules. It is worth noting that, although the loading capacity of the
440 hybrid microcapsules was different for each sample, the loading capacity of the
441 precursor liposomes was not statistically different (cf. Table 2) and thus the amount of
442 'liposomal curcumin' is expected to be similar in all capsules subjected to digestion.
443 Accordingly, no statistically significant differences were observed among the
444 microencapsulated samples. In this sense, incorporation of theoretical curcumin
445 contents greater than 1% in the precursor liposomes was considered impractical, as it
446 did not further improve the bioaccessibility of curcumin while it led to lower
447 encapsulation efficiencies.

448

449 **3.5. Protective effect of microencapsulation**

450 In order to assess whether the microencapsulation of curcumin within the proposed
451 system effectively stabilize the bioactive ingredient, the free and encapsulated
452 compound were dissolved/dispersed in PBS (pH=7.4) medium in which curcumin has
453 been described to be very unstable undergoing rapid hydrolytic degradation (Changguo
454 Chen, Thomas D Johnston, Hoonbae Jeon, Roberto Gedaly, Patrick P McHugh, Thomas
455 G Burke, et al., 2009). The optimal curcumin load determined from the previous
456 sections (i.e. 1% in the liposomes and 0.1% in the hybrid capsules) was selected for this

457 assay. Figure 3 shows the decay that its absorbance at 425 nm experienced in time due
458 to degradation.

459

460 INSERT FIGURE 3 ABOUT HERE

461

462 As expected, free curcumin rapidly degraded in PBS, being completely degraded in
463 only 1 h. In contrast, microencapsulated curcumin remained stable throughout the
464 experiment, showing minimal absorbance decay. The results also showed that
465 entrapment of curcumin within the liposomes was enough to greatly improve its
466 stability. However, a small absorbance drop was observed for liposomal curcumin
467 during the first hours, suggesting that the dual encapsulation approach provided
468 enhanced protection against degradation in the buffer. Although the protein concentrate
469 used in this work is water-dispersible, implying that the contents of the capsules would
470 be released upon dispersion of the powder in aqueous solution, whey proteins adsorb at
471 oil/water interfaces where they suffer conformational changes (Malaki Nik, Wright, &
472 Corredig, 2010; McClements, 2004), forming a film around the oil droplets which acts
473 as a physical barrier at the interface (Karaca, Low, & Nickerson, 2015; Zebib,
474 Mouloungui, & Noirot, 2010). As suggested above (cf. Section 3.2), this phenomenon
475 could also take place when the oil phase is organized into liposomes (Kasinos, Sabatino,
476 Vanloo, Gevaert, Martins, & Van der Meeren, 2013), explaining the additional
477 protective effect provided by the protein matrix, despite being water-dispersible. These
478 results are in agreement with those recently reported by Frenzel and co-workers (M.
479 Frenzel, Krolak, Wagner, & Steffen-Heins, 2015), who showed that whey protein

480 coatings increased the physical stability of soy phospholipids-based liposomes and
481 reduced their bilayer semi-permeability.

482

483 **4. Conclusions**

484 Novel food-grade hybrid encapsulation structures based on the entrapment of
485 phosphatidylcholine liposomes within a WPC matrix through electrospraying were
486 developed and used as delivery vehicles for curcumin. Liposomes produced by the
487 ethanol injection method were ultrasonicated to improve their electrosprayability by
488 reducing their size. Although relatively big (~400 nm) and polydisperse (PI~0.6),
489 liposomes produced at a lipid concentration as high as 80 g/L were successfully
490 incorporated within the WPC capsules. Entrapment of curcumin (1-8% w/w) within the
491 liposomes increased their size and reduced their stability, and the entrapment efficiency
492 of the liposomes decreased with increasing curcumin concentrations, suggesting that
493 their maximum curcumin loading capacity was 1-1.5 % (w/w). The excess curcumin
494 precipitated in the form of microcrystals, a fraction of which could be incorporated
495 together with the liposomal curcumin within the hybrid encapsulation structures upon
496 electrospraying of the WPC-liposome dispersions, increasing the loading capacity of
497 these vehicles despite the decrease in the encapsulation efficiency. Microencapsulation
498 of curcumin within the proposed hybrid structures significantly increased its
499 bioaccessibility (~1.7-fold) compared to the free compound, regardless of the curcumin
500 content in the capsules. Hence, incorporation of curcumin contents greater than 1% in
501 the liposomes was considered impractical, as the lower encapsulation efficiencies did
502 not compensate by an improvement in the bioaccessibility. Finally, the microcapsules
503 could successfully stabilize curcumin against degradation in PBS (pH = 7.4),

demonstrating that the whey protein coating of the liposomes obtained by the dual encapsulation strategy provided enhanced protection as compared to the simple entrapment within uncoated liposomes.

Acknowledgements

Laura G. Gómez-Mascaraque is recipient of a predoctoral contract from the Spanish Ministry of Economy and Competitiveness (MINECO), Call 2013. The authors would like to thank the Spanish MINECO projects AGL2012-30647 and AGL2015-63855-C2-1-R for financial support. Authors would also like to thank the Laboratory for Analytical Resources and Calibration (LRAC) at UNICAMP for the characterization services, and Prof. Dr. Rosiane Lopes da Cunha from the Laboratory of Process Engineering (UNICAMP) for granting the use of their equipment acquired from Fapesp Financil support (project numbers 2009/54137-1 and 2011/06083-0). Mariano Michelon and Allan Radaic are also gratefully acknowledged for technical and scientific support.

Appendix. Supplementary material

Supplementary material related to this article can be found in the Appendix.

Conflict of interest

The authors declare no conflict of interest.

References

Ahmed, K., Li, Y., McClements, D. J., & Xiao, H. (2012). Nanoemulsion- and emulsion-based delivery systems for curcumin: Encapsulation and release properties. *Food Chemistry, 132*(2), 799-807.

Cardoso, C., Afonso, C., Lourenço, H., Costa, S., & Nunes, M. L. (2015). Bioaccessibility assessment methodologies and their consequences for the risk–benefit evaluation of food. *Trends in Food Science & Technology, 41*(1), 5-23.

Chen, C., Johnston, T. D., Jeon, H., Gedaly, R., McHugh, P. P., Burke, T. G., & Ranjan, D. (2009). An in vitro study of liposomal curcumin: Stability, toxicity and biological activity in human lymphocytes and Epstein-Barr virus-transformed human B-cells. *International journal of pharmaceutics, 366*(1–2), 133-139.

Chen, C., Johnston, T. D., Jeon, H., Gedaly, R., McHugh, P. P., Burke, T. G., & Ranjan, D. (2009). An in vitro study of liposomal curcumin: stability, toxicity and biological activity in human lymphocytes and Epstein-Barr virus-transformed human B-cells. *International Journal of Pharmaceutics, 366*(1), 133-139.

Chin, D., Huebbe, P., Pallauf, K., & Rimbach, G. (2013). Neuroprotective Properties of Curcumin in Alzheimer's Disease. Merits and Limitations. *Current Medicinal Chemistry, 20*(32), 3955-3985.

de Freitas Zômpero, R. H., López-Rubio, A., de Pinho, S. C., Lagaron, J. M., & de la Torre, L. G. (2015). Hybrid encapsulation structures based on β-carotene-loaded nanoliposomes within electrospun fibers. *Colloids and Surfaces B: Biointerfaces, 134*, 475-482.

El Khoury, E. D., & Patra, D. (2013). Ionic liquid expedites partition of curcumin into solid gel phase but discourages partition into liquid crystalline phase of 1, 2-dimyristoyl-sn-glycero-3-phosphocholine liposomes. *The Journal of Physical Chemistry B, 117*(33), 9699-9708.

Feng, R., Zhu, W., Chu, W., Teng, F., Meng, N., Deng, P., & Song, Z. (2016). Y-shaped folic acid-conjugated PEG-PCL copolymeric micelles for delivery of curcumin. *Anti-Cancer Agents in Medicinal Chemistry, 16*.

Frenzel, M., Krolak, E., Wagner, A. E., & Steffen-Heins, A. (2015). Physicochemical properties of WPI coated liposomes serving as stable transporters in a real food matrix. *LWT - Food Science and Technology, 63*(1), 527-534.

Frenzel, M., & Steffen-Heins, A. (2015). Whey protein coating increases bilayer rigidity and stability of liposomes in food-like matrices. *Food Chemistry, 173*, 1090-1099.

Garti, N., & McClements, D. J. (2012). *Encapsulation technologies and delivery systems for food ingredients and nutraceuticals*: Elsevier.

Gómez-Mascaraque, L. G., Lagarón, J. M., & López-Rubio, A. (2015). Electrosprayed gelatin submicroparticles as edible carriers for the encapsulation of polyphenols of interest in functional foods. *Food Hydrocolloids, 49*(0), 42-52.

Gómez-Mascaraque, L. G., & López-Rubio, A. (2016). Protein-based emulsion electrosprayed micro- and submicroparticles for the encapsulation and stabilization of thermosensitive hydrophobic bioactives. *Journal of Colloid and Interface Science, 465*, 259-270.

Gómez-Mascaraque, L. G., Morfin, R. C., Pérez-Masiá, R., Sanchez, G., & Lopez-Rubio, A. (2016). Optimization of electrospraying conditions for the microencapsulation of probiotics and evaluation of their resistance during storage and in-vitro digestion. *LWT - Food Science and Technology, 69*, 438-446.

Gómez-Mascaraque, L. G., Sanchez, G., & López-Rubio, A. (2016). Impact of molecular weight on the formation of electrosprayed chitosan microcapsules as delivery vehicles for bioactive compounds. *Carbohydrate Polymers, 150*, 121-130.

Gómez-Mascaraque, L. G., Soler, C., & Lopez-Rubio, A. (2016). Stability and bioaccessibility of EGCG within edible micro-hydrogels. Chitosan vs. gelatin, a comparative study. *Food Hydrocolloids, 61*, 128-138.

Gültekin-Özgüven, M., Karadaı, A., Duman, Ş., Özkal, B., & Özçelik, B. (2016). Fortification of dark chocolate with spray dried black mulberry (Morus nigra) waste extract encapsulated in chitosan-coated liposomes and bioaccessability studies. *Food Chemistry, 201*, 205-212.

Hielscher, R., Wenz, T., Hunte, C., & Hellwig, P. (2009). Monitoring the redox and protonation dependent contributions of cardiolipin in electrochemically induced FTIR difference spectra of the cytochrome bc1 complex from yeast. *Biochimica et Biophysica Acta (BBA) - Bioenergetics, 1787*(6), 617-625.

Jaafar-Maalej, C., Diab, R., Andrieu, V., Elaissari, A., & Fessi, H. (2010). Ethanol injection method for hydrophilic and lipophilic drug-loaded liposome preparation. *Journal of liposome research, 20*(3), 228-243.

Karaca, A. C., Low, N., & Nickerson, M. (2015). Potential use of plant proteins in the microencapsulation of lipophilic materials in foods. *Trends in Food Science & Technology, 42*(1), 5-12.

Karadag, A., Özçelik, B., Sramek, M., Gibis, M., Kohlus, R., & Weiss, J. (2013). Presence of Electrostatically Adsorbed Polysaccharides Improves Spray Drying of Liposomes. *Journal of food science, 78*(2), E206-E221.

Karewicz, A., Bielska, D., Gzyl-Malcher, B., Kepczynski, M., Lach, R., & Nowakowska, M. (2011). Interaction of curcumin with lipid monolayers and liposomal bilayers. *Colloids and Surfaces B: Biointerfaces, 88*(1), 231-239.

Kasinos, M., Sabatino, P., Vanloo, B., Gevaert, K., Martins, J. C., & Van der Meeren, P. (2013). Effect of phospholipid molecular structure on its interaction with whey proteins in aqueous solution. *Food Hydrocolloids, 32*(2), 312-321.

Laye, C., McClements, D. J., & Weiss, J. (2008). Formation of Biopolymer-Coated Liposomes by Electrostatic Deposition of Chitosan. *Journal of food science, 73*(5), N7-N15.

Liu, W., Zhai, Y., Heng, X., Che, F. Y., Chen, W., Sun, D., & Zhai, G. (2016). Oral bioavailability of curcumin: problems and advancements. *Journal of Drug Targeting*, 1-9.

Liu, Y., Liu, D., Zhu, L., Gan, Q., & Le, X. (2015). Temperature-dependent structure stability and in vitro release of chitosan-coated curcumin liposome. *Food Research International, 74*, 97-105.

López-Rubio, A., & Lagaron, J. M. (2012). Whey protein capsules obtained through electrospraying for the encapsulation of bioactives. *Innovative Food Science & Emerging Technologies, 13*(0), 200-206.

Malaki Nik, A., Wright, A. J., & Corredig, M. (2010). Interfacial design of protein-stabilized emulsions for optimal delivery of nutrients. *Food & function, 1*(2), 141-148.

McClements, D. J. (2004). Protein-stabilized emulsions. *Current Opinion in Colloid & Interface Science, 9*(5), 305-313.

Ndong Ntoutoume, G. M. A., Granet, R., Mbakidi, J. P., Brégier, F., Léger, D. Y., Fidanzi-Dugas, C., Lequart, V., Joly, N., Liagre, B., Chaleix, V., & Sol, V. (2016). Development of curcumin–cyclodextrin/cellulose nanocrystals complexes: New anticancer drug delivery systems. *Bioorganic & Medicinal Chemistry Letters, 26*(3), 941-945.

Nelson, K. M., Dahlin, J. L., Bisson, J., Graham, J., Pauli, G. F., & Walters, M. A. (2017). The Essential Medicinal Chemistry of Curcumin. *Journal of Medicinal Chemistry, 60*(5), 1620-1637.

Patra, D., El Khoury, E., Ahmadieh, D., Darwish, S., & Tafech, R. M. (2012). Effect of Curcumin on Liposome: Curcumin as a Molecular Probe for Monitoring Interaction of Ionic Liquids with 1, 2-Dipalmitoyl-sn-Glycero-3-Phosphocholine Liposome. *Photochemistry and photobiology, 88*(2), 317-327.

626 Pérez-Masiá, R., Lagaron, J., & Lopez-Rubio, A. (2015). Morphology and Stability of Edible
627 Lycopene-Containing Micro- and Nanocapsules Produced Through Electrospraying and
628 Spray Drying. *Food and Bioprocess Technology, 8*(2), 459-470.
629 Pérez-Masiá, R., López-Nicolás, R., Periago, M. J., Ros, G., Lagaron, J. M., & López-Rubio, A.
630 (2015). Encapsulation of folic acid in food hydrocolloids through nanospray drying and
631 electrospraying for nutraceutical applications. *Food Chemistry, 168*, 124-133.
632 Qian, C., Decker, E. A., Xiao, H., & McClements, D. J. (2012). Nanoemulsion delivery systems:
633 Influence of carrier oil on β-carotene bioaccessibility. *Food Chemistry, 135*(3), 1440-
634 1447.
635 Schneider, C., Gordon, O. N., Edwards, R. L., & Luis, P. B. (2015). Degradation of Curcumin:
636 From Mechanism to Biological Implications. *Journal of Agricultural and Food*
637 *Chemistry, 63*(35), 7606-7614.
638 Sipoli, C. C., Santana, N., Shimojo, A. A. M., Azzoni, A., & de la Torre, L. G. (2015). Scalable
639 production of highly concentrated chitosan/TPP nanoparticles in different pHs and
640 evaluation of the in vitro transfection efficiency. *Biochemical Engineering Journal, 94*,
641 65-73.
642 Snowman, J. W. (1988). Downstream Processes: Equipment and Techniques. Alan R. Liss. *Inc.,*
643 *New York*, 315-351.
644 Tan, C., Feng, B., Zhang, X., Xia, W., & Xia, S. (2016). Biopolymer-coated liposomes by
645 electrostatic adsorption of chitosan (chitosomes) as novel delivery systems for
646 carotenoids. *Food Hydrocolloids, 52*, 774-784.
647 Van Den Hoven, J. M., Metselaar, J. M., Storm, G., Beijnen, J. H., & Nuijen, B. (2012).
648 Cyclodextrin as membrane protectant in spray-drying and freeze-drying of PEGylated
649 liposomes. *International Journal of Pharmaceutics, 438*(1-2), 209-216.
650 Wang, L., Hu, X., Shen, B., Xie, Y., Shen, C., Lu, Y., Qi, J., Yuan, H., & Wu, W. (2015). Enhanced
651 stability of liposomes against solidification stress during freeze-drying and spray-drying
652 by coating with calcium alginate. *Journal of Drug Delivery Science and Technology, 30*,
653 163-170.
654 Yamaguchi, T., Nomura, M., Matsuoka, T., & Koda, S. (2009). Effects of frequency and power of
655 ultrasound on the size reduction of liposome. *Chemistry and Physics of Lipids, 160*(1),
656 58-62.
657 Zebib, B., Mouloungui, Z., & Noirot, V. (2010). Stabilization of Curcumin by Complexation with
658 Divalent Cations in Glycerol/Water System. *Bioinorganic Chemistry and Applications,*
659 *2010*, 8.

660

Tables

Table 1. Average size and polydispersity index (PDI) of unloaded liposomes prepared with different lipid concentrations (a), and curcumin-loaded liposomes prepared with 80 g/L lipids (b)

a) Unloaded liposomes			b) Curcumin-loaded liposomes		
[lipid] (g/L)	**Average hydrodynamic diameter (nm)**	**PDI**	**[curcumin] (% w/w)**	**Average hydrodynamic diameter (nm)**	**PDI**
20	206 ± 3	0.27 ±	**0**	407 ± 58	0.66 ± 0.06
40	244 ± 3	0.43 ±	**1**	508 ± 46	0.75 ± 0.02
60	342 ± 38	0.59 ±	**2**	656 ± 188	0.73 ± 0.04
80	407 ± 58	0.66 ±	**8**	771 ± 54	0.87 ± 0.07

Table 2. Entrapment or encapsulation efficiency and loading capacity of curcumin-loaded liposomes (a) and curcumin-loaded hybrid microcapsules (b)

a) Liposomes			b) Hybrid microcapsules		
[curcumin] (% w/w)	**EE (%)**	**LC (%)**	**[curcumin] (% w/w)**	**EE (%)**	**LC (%)**
1	79 ± 1 [a]	0.79 ± 0.01	**0**	-	-
2	72 ± 3 [a]	1.44 ± 0.07	**0.1**	104 ± 5 [a]	0.104 ±
4	32 ± 10 [b]	1.27 ± 0.43	**0.2**	75 ± 1 [b]	0.150 ±
8	11 ± 1 [b]	0.87 ± 0.05	**0.4**	69 ± 4 [b]	0.275 ±

Different letters (a–c) within the same column indicate significant differences at $p<0.05$ among the samples

Table 3. Bioaccessibility of pure and microencapsulated curcumin

Sample – $[curcumin]_{theoretical}$	**Bioaccessibility (%)**
Free curcumin - pure	3.2 ± 0.5 [a]
Microcapsules - 0.1% w/w	5.4 ± 0.5 [b]
Microcapsules - 0.2% w/w	5.3 ± 0.5 [b]
Microcapsules - 0.4% w/w	4.8 ± 0.3 [b]

Different letters (a–b) within the same column indicate significant differences at $p<0.05$ among the samples

FIGURE CAPTIONS

Figure 1. SEM images and particle size distributions of unloaded hybrid encapsulation structures obtained with different liposome concentrations: a) 0% lipid, b) 2.5% lipid, c) 5% lipid, d) 7.5% lipid and e) 10% lipid; f) FT-IR spectra of commercial lipids, electrosprayed WPC and the liposome-WPC hybrid carriers.

Figure 2. Thermograms of unloaded and curcumin-loaded liposomes with different curcumin w/w concentrations (a) and variation of their transition temperature (pointed by the arrow) with the theoretical concentration of curcumin (b). The dotted line is only for visual guidance purposes.

Figure 3. Degradation profiles for free and encapsulated curcumin in PBS (pH=7.4).

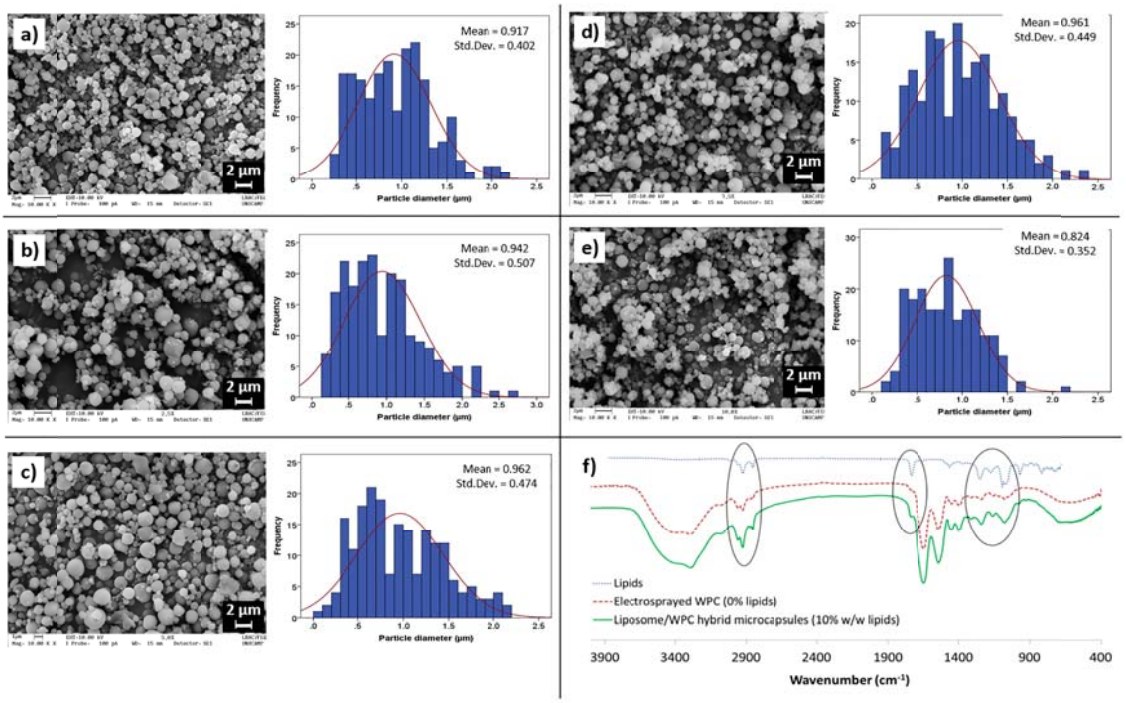

686

687

688 FIGURE 1.

689

690 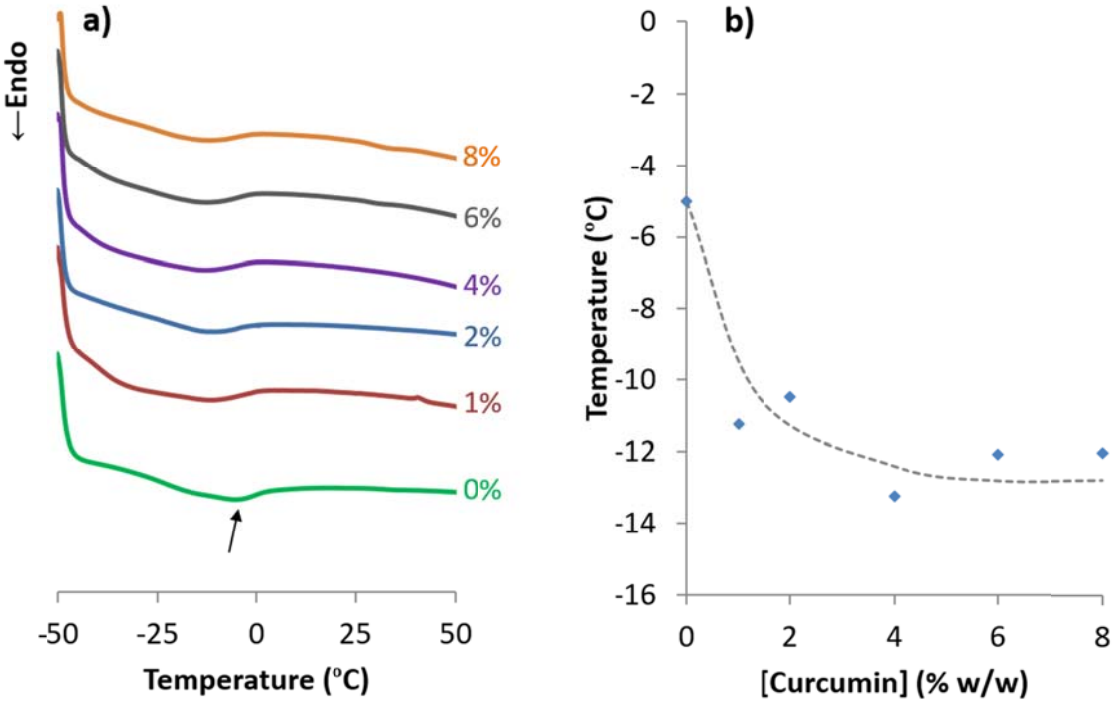

691

692 FIGURE 2.

693

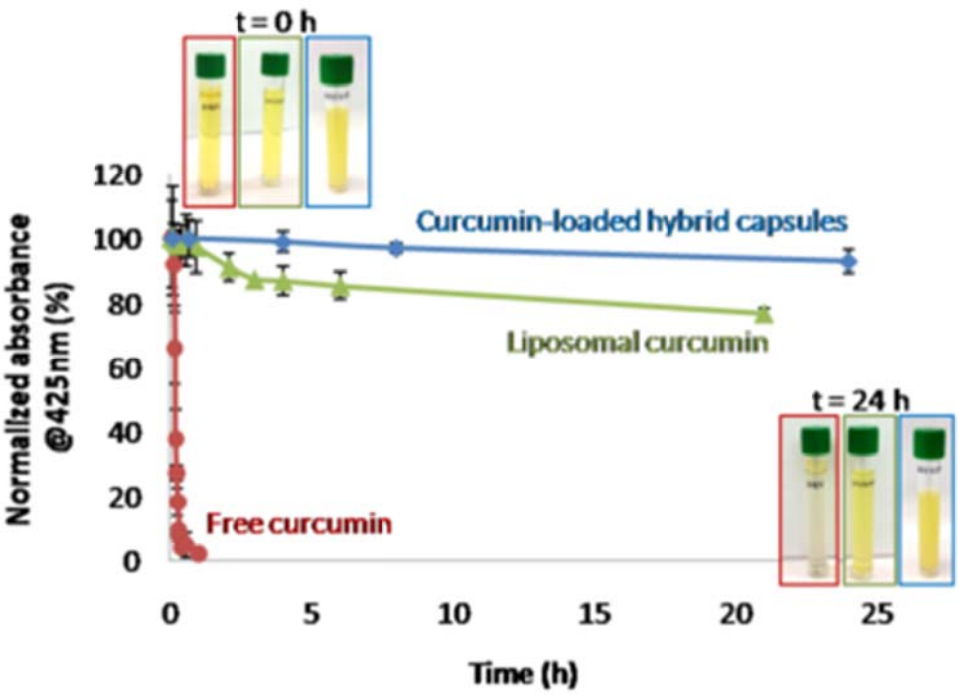

694

695 FIGURE 3.

696

Supplementary material

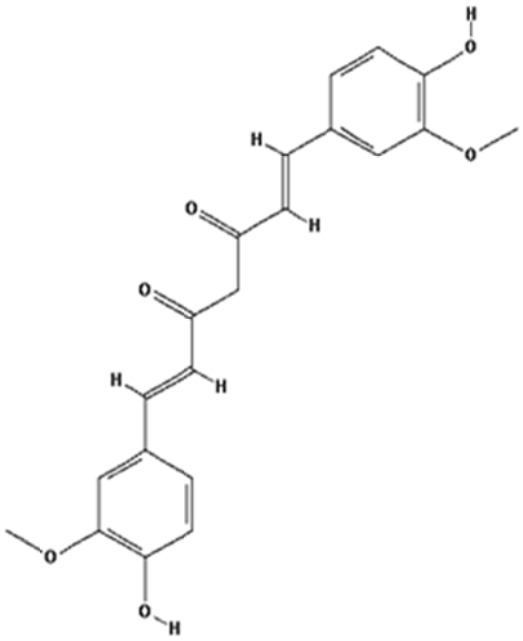

Figure S1. Molecular structure of curcumin. Source: National Center for Biotechnology Information. PubChem Compound Database; CID=969516, https://pubchem.ncbi.nlm.nih.gov/compound/969516.

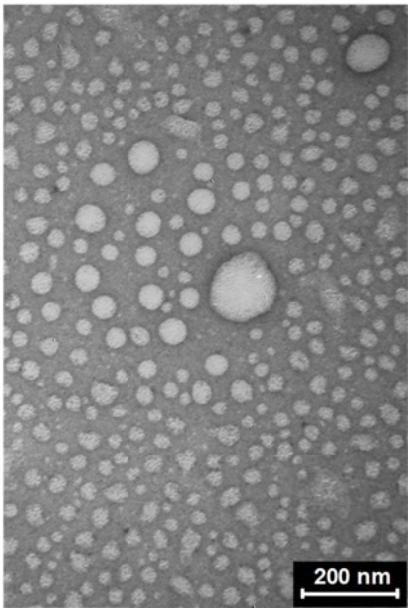

Figure S2. TEM image of liposomes prepared through the ethanol injection method followed by ultrasound treatment, with a final lipid concentration of 80 g/L.

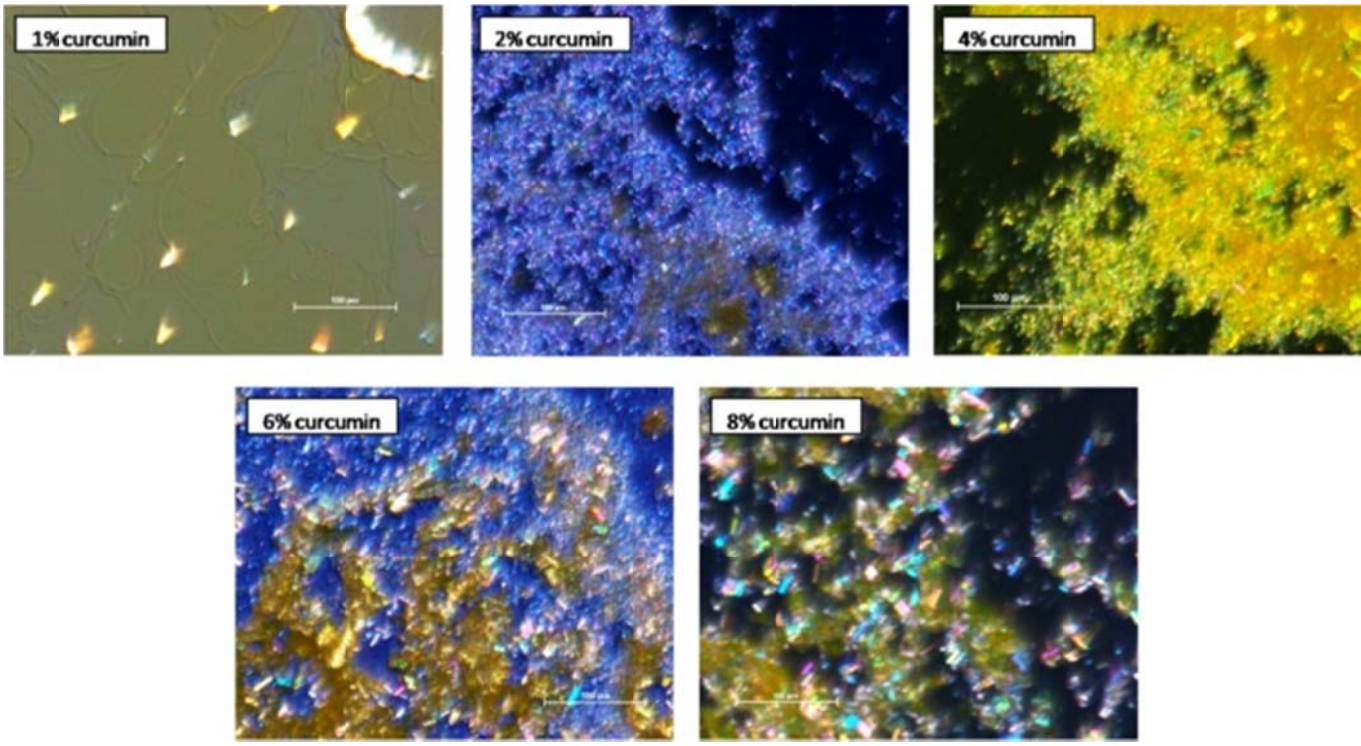

Figure S3. Images obtained by polarized-light microscopy of the centrifugate from curcumin-loaded liposome suspensions with different curcumin contents. Scale bars indicate 100 µm.

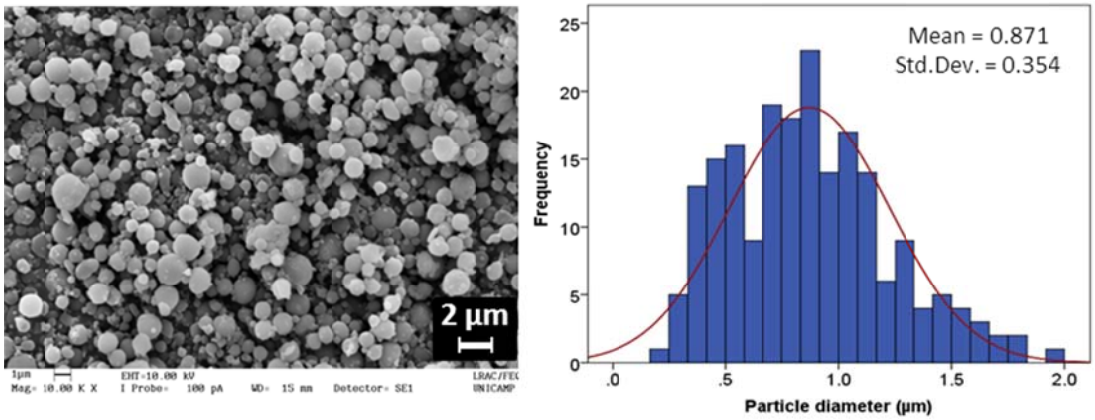

Figure S4. SEM image of curcumin-loaded hybrid encapsulation structures with theoretical curcumin concentration of 0.2% w/w (left) and their particle size distribution (right).